Inhibitor binding studies on enoyl-reductase reveal conformational changes related to substrate recognition.

Roujeinikova, A.; Sedelnikova, S.; de Boer, G.J.; Stuitje, A.R.; Slabas, A.R.; Rafferty, J.B.; Rice, D.W.

published in
Journal of Biological Chemistry
1999

DOI (link to publisher)
10.1074/jbc.274.43.30811

document version
Publisher's PDF, also known as Version of record

THE JOURNAL OF BIOLOGICAL CHEMISTRY
Vol. 274, No. 43, Issue of October 22, pp. 30811–30817, 1999

Printed in U.S.A.

Inhibitor Binding Studies on Enoyl Reductase Reveal Conformational Changes Related to Substrate Recognition*

(Received for publication, April 23, 1999, and in revised form, June 25, 1999)

Anna Roujeinikova‡, Svetlana Sedelnikova‡, Gert-Jan de Boer§¶, Antoine R. Stuitje§, Antoni R. Slabas‖, John B. Rafferty‡, and David W. Rice‡ ‡‡**

From the ‡Krebs Institute for Biomolecular Research, Department of Molecular Biology and Biotechnology, University of Sheffield, Sheffield S10 2TN, United Kingdom, the §Department of Genetics, Institute of Molecular Biological Studies, Vrije Universiteit, Biocenter Amsterdam, 1081 HV Amsterdam, The Netherlands, and the ‖Department of Biological Sciences, University of Durham, Durham DH1 3LE, United Kingdom

Enoyl acyl carrier protein reductase (ENR) is involved in fatty acid biosynthesis. In *Escherichia coli* this enzyme is the target for the experimental family of antibacterial agents, the diazaborines, and for triclosan, a broad spectrum antimicrobial agent. Biochemical studies have suggested that the mechanism of diazaborine inhibition is dependent on NAD^+ and not NADH, and resistance of *Brassica napus* ENR to diazaborines is thought to be due to the replacement of a glycine in the active site of the *E. coli* enzyme by an alanine at position 138 in the plant homologue. We present here an x-ray analysis of crystals of *B. napus* ENR A138G grown in the presence of either NAD^+ or NADH and the structures of the corresponding ternary complexes with thienodiazaborine obtained either by soaking the drug into the crystals or by co-crystallization of the mutant with NAD^+ and diazaborine. Analysis of the ENR A138G complex with diazaborine and NAD^+ shows that the site of diazaborine binding is remarkably close to that reported for *E. coli* ENR. However, the structure of the ternary ENR A138G-NAD^+-diazaborine complex obtained using co-crystallization reveals a previously unobserved conformational change affecting 11 residues that flank the active site and move closer to the nicotinamide moiety making extensive van der Waals contacts with diazaborine. Considerations of the mode of substrate binding suggest that this conformational change may reflect a structure of ENR that is important in catalysis.

Enoyl acyl carrier protein reductase (ENR)[1] is a key component of type II fatty acid synthetase, which is found in both plants and bacteria (1). It catalyzes the second reductive step in the fatty acid biosynthesis pathway, converting a *trans*-2,3 enoyl moiety into a saturated acyl chain, and utilizes NAD(P)H as a cofactor. The study of this enzyme as a drug target has recently received increased attention in connection with the discovery that three distinctly different synthetic anti-bacterial drugs, isoniazid (2), diazaborine (3, 4), and triclosan (5, 6) block lipid biosynthesis in bacteria by inhibiting ENR. The recent structural studies on diazaborine-bound *Escherichia coli* ENR (7) elucidated the mechanism by which diazaborine inhibits bacterial ENR and also threw light onto the molecular nature of the *E. coli* ENR G93S mutant's resistance to diazaborines (8). These studies indicate that a $Gly^{93} \rightarrow Ser$ substitution puts the larger amino acid side chain at the position where it would clash with the sulfonyl oxygens of the diazaborine molecule. The *Brassica napus* and the *E. coli* enoyl reductases share 35% sequence identity, and structural comparison of the two enzymes has shown that the amino acid residues forming the active site are highly conserved between the two proteins (7, 9). However, in contrast to the *E. coli* enzyme, *B. napus* ENR is insensitive to diazaborine (4). Molecular genetic and biochemical studies on mutants of *B. napus* ENR (10) have suggested that the presence of an alanine residue at position 138 of *B. napus* ENR (structurally equivalent to position 93 in the *E. coli* enzyme) is the major determinant for its resistance to diazaborine. Furthermore, kinetic studies on *E. coli* ENR and *B. napus* ENR A138G (4, 10) have shown that, although diazaborine inhibits ENR in the presence of NAD^+, the compound's inhibitory activity with NADH is hardly detectable.

In order to analyze the molecular basis of resistance and sensitivity to diazaborine of *B. napus* ENR and to assess the role of the oxidized and reduced forms of the cofactor in the formation of the enzyme-nucleotide-diazaborine complexes, we have determined and analyzed the x-ray crystal structures of the A138G mutant of *B. napus* ENR complexed with either NAD^+ or NADH both in the presence and absence of thienodiazaborine. In this paper we report the results of this analysis and also compare the effect of producing these complexes by soaking *versus* co-crystallization, which reveals a conformational change on drug binding that we presume to be linked to substrate recognition.

EXPERIMENTAL PROCEDURES

Preparation of Crystal Complexes

The diazaborine-sensitive *B. napus* ENR A138G mutant has an enzymatic activity closely related to that of the wild type enzyme and was prepared as described previously (10). Co-crystallization of ENR A138G with either oxidized or reduced form of the cofactor was conducted using 4-μl drops containing 15 mg/ml (0.45 mM) ENR A138G, 1.5 mM NAD^+ or NADH in either 0.05 M MES, pH 6.0, for NAD^+ or 0.05 M HEPES, pH 8.0, for NADH, mixed with the same volume of the reser-

* This work was supported in part by grants from the Biotechnology and Biological Sciences Research Council, the Wellcome Trust, and New Energy and Industrial Technology Development Organization. The costs of publication of this article were defrayed in part by the payment of page charges. This article must therefore be hereby marked "*advertisement*" in accordance with 18 U.S.C. Section 1734 solely to indicate this fact.

The atomic coordinates and structure factors (code 1CWU) have been deposited in the Protein Data Bank, Research Collaboratory for Structural Bioinformatics, Rutgers University, New Brunswick, NJ (http://www.rcsb.org/).

¶ Present address: Dept. of Plant Biology, Carnegie Institution of Washington, Stanford, CA 94305.

** BBSRC David Phillips Research Fellow.

‡‡ To whom all correspondence should be addressed: Krebs Inst. for Biomolecular Research, Dept. of Molecular Biology and Biotechnology, University of Sheffield, Firth Court, Western Bank, Sheffield S10 2TN, United Kingdom. Tel.: 44-114-222-4242; Fax: 44-114-272-8697; E-mail: d.rice@sheffield.ac.uk.

[1] The abbreviations used are: ENR, enoyl acyl carrier protein reductase; MES, 2-(N-morpholino)ethanesulfonic acid; SDMS, San Diego multiwire systems, CoA, coenzyme A; PDB, Protein Data Bank.

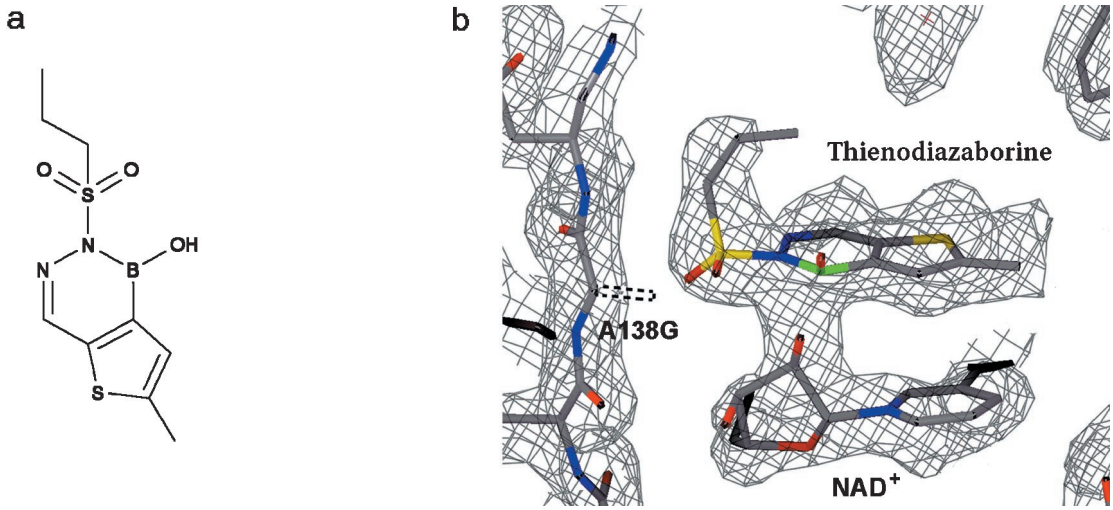

FIG. 1. *a*, chemical structure of thienodiazaborine used in the present study. *b*, the Fourier map of the refined model for the ENR A138G-NAD^+-thienodiazaborine complex, obtained by soaking the drug into the crystals of the NAD^+-bound ENR A138G, at 2.1-Å resolution with the final refined structure superimposed. The density was calculated with coefficients $(2F_o - F_c)$ and contoured at 1 σ. There was no interpretable electron density for the terminal methyl group of the propyl moiety of the thienodiazaborine. The boron atom of diazaborine is colored *green* (the covalent linkage between this atom and the 2′ hydroxyl of the nicotinamide ribose is not shown). The mutated residue (A138G) is labeled, and the position of the C_β of the Ala^{138} side chain, as observed in the wild type diazaborine-insensitive enzyme, is shown with a *dashed line* (produced using O; Ref. 22).

voir solution containing 1.8 M $(NH_4)_2SO_4$ and 0.1 M of the appropriate buffer, and equilibrated against the reservoir solution at 17 °C. The crystals are isomorphous to those of the wild type enzyme and belong to the space group $P4_22_12$ with cell dimensions $a = b = 70.5$ Å, $c = 117.5$ Å for the NAD^+ complex ($c = 117.7$ Å for the NADH complex), and with a monomer in the asymmetric unit. Ternary complexes of ENR A138G (containing the cofactor and thienodiazaborine) were obtained both by soaking and co-crystallization experiments. The soaking of the inhibitor into the "binary" crystals was conducted for 4 h using a stabilizing solution containing 5 mM thienodiazaborine and 3 mM NAD^+ or NADH. Co-crystallization experiments were conducted in hanging drops, containing 7.5 mg/ml ENR A138G, 1.5 mM NAD^+, 0.75 mM thienodiazaborine, 2.25 M NaCl and 50 mM sodium acetate, pH 5.3, suspended over a well solution containing 4.5 M NaCl and 50 mM sodium acetate, pH 5.3. The latter crystals represent a new crystal form (hereafter referred to as form B) and belong to the space group $I4_122$ with cell dimensions $a = b = 104.6$ Å, $c = 284.0$ Å and with a dimer in the asymmetric unit.

X-ray Data Collection

X-ray diffraction data for both the binary complexes as well as for the diazaborine-soaked crystals were collected at room temperature on a twin San Diego multiwire systems (SDMS) area detector with Rigaku RU-200 rotating anode source. The data were processed and merged using SDMS software (11). X-ray diffraction data for the form B crystal complex were collected from a crystal cooled to 100 K using an Oxford Cryosystems Cryostream device to 2.5 Å on a MAR image plate detector on station 9.6 at the Synchrotron Radiation Source Daresbury Laboratory. A cryoprotectant solution contained 20% glycerol, 3.7 M NaCl, 3 mM NAD^+, 1.5 mM thienodiazaborine, and 50 mM sodium acetate, pH 5.3. The data were processed using the DENZO/SCALEPACK package (12). A summary of the data-processing statistics is presented in Table I. Subsequent data handling employed the CCP4 program suite (13).

Structure Determination and Refinement

Binary ENR A138G-NAD(H) Complexes—The same procedure was applied in building the models for both of the binary complexes. The starting coordinates were those of the wild type *B. napus* ENR complex with NAD^+ (Protein Data Bank (PDB) code 1eno) or NADH (PDB code 1enp) (14) with Ala^{138} replaced by Gly, and the cofactor and all waters excluded. These models were used to calculate initial electron density $(2F_{obs} - F_{calc})$ and $(F_{obs} - F_{calc})$ maps, which showed readily interpretable electron density either for the reduced or for the oxidized form of the cofactor. In case of the NAD^+-complex, the electron density in the region of the nicotinamide ring, its associated ribose, and the pyrophosphate moiety was very weak. The cofactors were incorporated into the respective models, which were then submitted to rounds of restrained positional and isotropic B-factor refinement using the TNT program (15), including a correction for the solvent continuum (16). The structures were rebuilt where necessary using the FRODO program (17). Water molecules were introduced during the course of the refinement at geometrically reasonable positions, but those with the refined value of the B-factor above 70 $Å^2$ were deleted from the coordinate list. Analysis of the stereochemical quality of the models was accomplished using the PROCHECK program (18). Refinement statistics are summarized in Table I.

Ternary ENR A138G-NAD(H)-Diazaborine Complexes Obtained by Soaking—For each of the ternary complexes obtained by soaking, the starting coordinates were those of the respective binary complex with the cofactor and all waters excluded. These models were used to calculate initial electron density $(2F_{obs} - F_{calc})$ and $(F_{obs} - F_{calc})$ maps, which in both cases clearly showed the position of the diazaborine and a cofactor in the active site of ENR A138G. Both cofactor and inhibitor molecules were incorporated into the models, which were then submitted to the refinement procedure that was essentially the same as described for the binary complexes. Refinement statistics are presented in Table I.

ENR A138G-NAD^+-Diazaborine Complex Obtained by Co-crystallization—Since the crystallization of ENR A138G in the presence of NAD^+ and thienodiazaborine led to the appearance of a previously unobserved crystal form (form B), the structure was solved by molecular replacement using a search model based on a dimer of the ternary ENR A138G-NAD^+-diazaborine complex, produced by soaking the drug into crystals, with the cofactor, diazaborine, and all waters excluded. Molecular replacement was performed using the AMORE program (19). The rotation function yielded one hit that was clearly above the others ($\alpha = 39°$, $\beta = 90°$, $\gamma = 281°$). This top hit was then used in a translation search. The top hit from the translation function ($TF = 19.7$ σ, fractional translation parameters $tx = 0.122$, $ty = 0.596$, $tz = 0.048$) was then rigid-body refined from a starting R-value of 0.41 to 0.35 using data in the range 10–3.5 Å. The resultant electron density maps with coefficients $(2F_o - F_c)$ and $(F_o - F_c)$ at 2.5 Å showed clear density for the NAD^+ molecules bound in the active site of each monomer as well as density for the inhibitor. Inspection of electron density maps in the region of the enzyme active site also revealed a substantial conformational change for the part of the chain comprising residues 236–246 in both of the subunits. These residues were moved to the correct positions indicated by an omit map, and the NAD^+ and diazaborine molecules were also incorporated into the model. Following restrained positional refinement of the atomic coordinates with all B-factors fixed at 25 $Å^2$, the R-factor of the model dropped to 0.299 for data in the range 10–2.5 Å. From then on, the structure was refined by successive cycles consisting of restrained positional and isotropic B-factor refinement, including a correction for solvent continuum followed by manual rebuilding using the FRODO program. Water molecules were introduced during the course of the refinement at geometrically reasonable positions, but these only retained upon refinement if their B-factors remained below 60 $Å^2$. Refinement statistics are summarized in Table I.

TABLE I
Crystallographic data

ENR A138G crystal complex	NAD^+	NADH	NAD^+, diazaborine (soaking)	NADH, diazaborine (soaking)	NAD^+, diazaborine (form B)
X-ray data collection statistics					
Resolution limit (Å)	2.1	2.0	2.1	2.4	2.5
No. of observed reflections	69,587	76,971	52,166	47,298	90,629
No. of unique reflections	18,081	18,245	16,038	10,933	25,755
Completeness (outer shell) (%)	94 (74)	88 (88)	85 (63)	87 (67)	93 (93)
R_{merge}[a] (outer shell)	0.051 (0.165)	0.076 (0.217)	0.051 (0.180)	0.086 (0.220)	0.057 (0.188)
Refinement statistics					
Resolution (Å)	10–2.1	10–2.0	10–2.1	10–2.4	10–2.5
No. of reflections used	17,154	17,346	15,218	10,354	24,431
R_{cryst}[b]	0.160	0.158	0.164	0.174	0.211
R_{free}[c]	0.209	0.207	0.229	0.242	0.314
No. of solvent molecules	103	108	94	76	113
Bond-length rms deviation (Å)	0.013	0.010	0.011	0.011	0.012
Bond-angle rms deviation (°)	1.7	1.5	1.5	1.7	1.4
Ramachandran plot (%)[d]	92 (8)	92 (8)	93 (7)	92 (8)	90 (10)
Average B (protein) (Å^2)	22	29	21	24	32
Average B (cofactor) (Å^2)	75	42	37	46	30
Average B (diazaborine) (Å^2)			37	51	24

[a] $R_{merge} = \Sigma_{hkl}|I_j - I_m|/\Sigma_{hkl}I_m$, where I_j and I_m are the observed intensity and mean intensity of related reflections, respectively.
[b] $R_{cryst} = \Sigma_{hkl}(||F_{obs}| - |F_{calc}||)/\Sigma_{hkl}|F_{obs}|$.
[c] R_{free} was calculated on 5% of the data omitted at random.
[d] The percentage of non-glycine and non-proline residues falling within the most favored and allowed regions (in parentheses).

RESULTS AND DISCUSSION

Analysis of the Structures of the Binary Complexes—The ENR A138G mutant crystallizes in the presence of both the oxidized and reduced forms of the cofactor isomorphously to the corresponding binary wild type enzyme complexes (14). Therefore, the structures of both the binary complexes were solved directly by refinement starting from the corresponding coordinates of the binary complexes of the wild type enzyme (see "Experimental Procedures"). For both the complexes, the overall protein structure was found to be essentially identical to that of the wild type enzyme and no structural rearrangements were observed in the vicinity of the mutation. Like in the structure of the wild type ENR-NAD^+ complex, the electron density for the NAD^+ in the mutant enzyme was good for the adenine ring and its associated ribose sugar, very poor for the pyrophosphate moiety, and there was no interpretable density for the nicotinamide moiety and its associated ribose sugar, consistent with the temperature factor for these parts of the cofactor molecule reaching the upper cut-off limit of 100 Å^2 during refinement. In the ENR A138G-NADH complex, the density for the entire NADH molecule was readily interpretable, although that for the pyrophosphate moiety was somewhat less well defined. The location and the extended conformation for the NADH molecule with both ribose sugars being in C2′-*endo* conformation was found to be very similar to that described for the corresponding wild type ENR binary complex (14). Comparison of the structures of ENR A138G with NAD^+ and NADH bound shows that the only major difference in the conformation of the protein occurs in the position of the side chain of Tyr^{32}. In the NAD^+-bound structure, this residue adopts a well defined conformation and occupies part of the binding pocket for the nicotinamide moiety. In the NADH-bound ENR A138G structure, the side chain of Tyr^{32} moves so that the volume of the binding pocket increases compared with the complex with NAD^+, allowing the reduced nicotinamide ring to occupy the binding site where it is stabilized by van der Waals contact with the edge of the phenolic ring of the tyrosine. This situation is equivalent to the structural change that occurs on NADH *versus* NAD^+ binding with the wild type enzyme.

Location of the Diazaborine Binding Site in the Crystals of ENR A138G Grown in the Presence of NAD^+ or NADH—Previous enzyme inhibition assays on *E. coli* ENR and *B. napus* ENR A138G (4, 10), which followed the oxidation of NADH in the presence or absence of diazaborine, have been carried out using crotonyl-CoA as a substrate. These kinetic studies showed that, whereas the initial velocity of the reaction was hardly affected by diazaborine, the inhibitory effect increased during the course of the reaction, pointing to the involvement of a reaction product, NAD^+, rather than NADH, in the mechanism of diazaborine inhibition.

However, our experiments on soaking thienodiazaborine (Fig. 1*a*) into the "binary" crystals of ENR A138G with NAD^+ or NADH produced electron density maps for both complexes, which are qualitatively very similar and show clear electron density for the entire cofactor and the drug in both structures. Thus, binding of diazaborine to the ENR A138G-NAD^+ complex has resulted in the ordering on the enzyme surface of those parts of the NAD^+ molecule that are disordered in the binary complex. In addition, the movement of Tyr^{32} associated with localizing the nicotinamide ring, which had previously only been observed in the structure of the binary complex with NADH, was also seen. Analysis of the structure of the complex obtained through soaking crystals of the binary complex with NADH in diazaborine shows no features different from the complex with NAD^+ and diazaborine.

In both structures, thienodiazaborine stacks onto the nicotinamide ring of the cofactor (Fig. 1b) and makes further van der Waals contacts with the side chains of Tyr^{188}, Met^{202}, Lys^{206}, Ile^{244}, and Ile^{247} and with the main-chain peptide between Gly^{138} and Gly^{140}. The boron hydroxyl forms a hydrogen bond with the phenolic hydroxyl of Tyr^{198}. Of considerable importance in stabilizing the diazaborine in the active site are extensive π-π stacking interactions formed between the bicyclic rings of the diazaborine and the nicotinamide ring. The stacking involves only partial overlap of the rings so that the carbamide group of the nicotinamide moiety forms close contact with the adjacent ring system. This stacking interaction is closely related to that observed in the *E. coli* ENR-NAD^+-diazaborine complex (7).

In the structures of the *B. napus* ENR A138G complexes with either the oxidized or reduced form of the cofactor and thienodiazaborine, the boron atom of the drug and the 2′ hydroxyl of the nicotinamide ribose are clearly covalently linked, and the

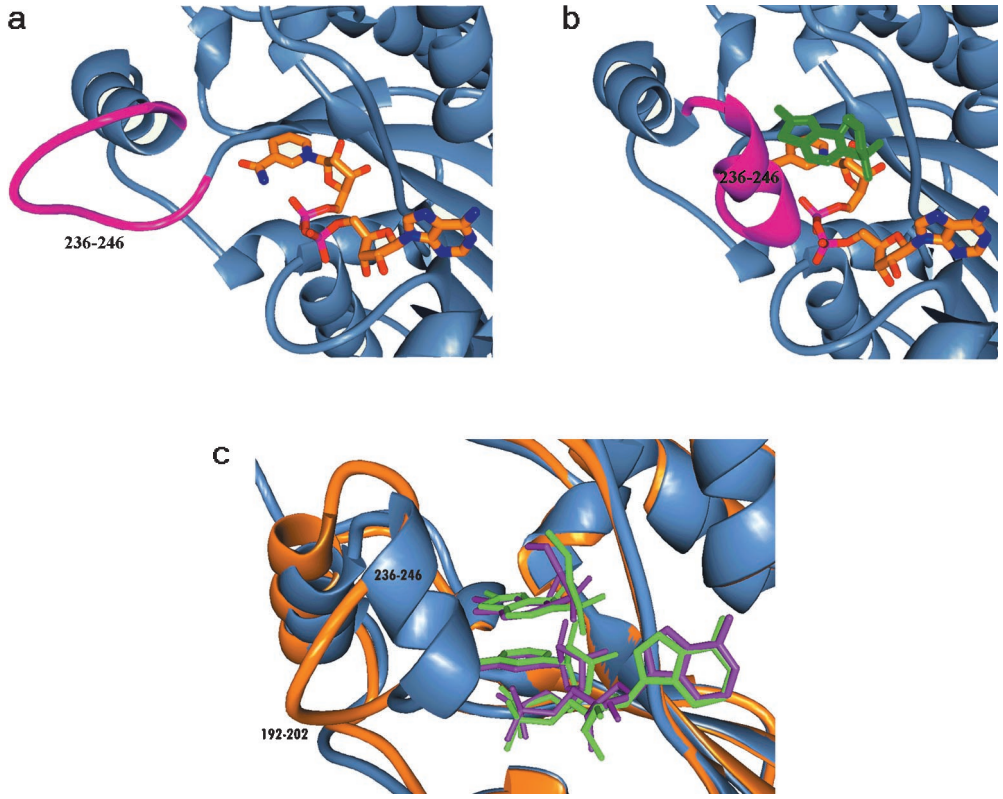

FIG. 2. *a*, ribbon representation of the ENR A138G-NADH binary complex in the region of the active site. Residues 236–246 are shown in *magenta*. *b*, ribbon representation of the ENR A138G-NAD^+-thienodiazaborine ternary complex, obtained by co-crystallization, in the same view as in *a*. The diazaborine molecule is drawn in *green*. Residues 236–246 are shown in *magenta*, and the shift in position of this loop compared with that seen in the binary complex with NADH is evident. *c*, ribbon diagram of the *E. coli* ENR-NAD^+-thienodiazaborine complex (PDB code 1dfh) superimposed on the *B. napus* ENR A138G-NAD^+-thienodiazaborine complex, obtained by co-crystallization. The diagram illustrates the remarkably similar mode of diazaborine binding. The backbone atoms are shown in *blue* for *B. napus* ENR A138G and *orange* for *E. coli* ENR. The NAD^+ and the diazaborine molecules bound to *B. napus* ENR A138G are colored *green*; those bound to *E. coli* ENR are *magenta*. The equivalent loops 192–202 (*E. coli* ENR) and 236–246 (*B. napus* ENR A138G) are labeled, and their difference in position is clear. *d*, stereoview of the diazaborine-binding sites of the superimposed *B. napus* ENR A138G-NAD^+-thienodiazaborine complex, obtained by co-crystallization, and *E. coli* ENR-NAD^+-thienodiazaborine complex. The diazaborine and the nicotinamide moiety and its associated ribose are shown only for the *B. napus* ENR ternary complex, in ball-and-stick representation with carbon atoms colored *gray*, nitrogen *blue*, sulfur *yellow*, oxygen *red*, and boron *orange*. For clarity, only the key residues responsible for diazaborine binding are shown, and the rest of the chains are drawn schematically in thin lines. *B. napus* ENR is drawn in *magenta* and *E. coli* ENR in *green*. Residues are labeled in *B. napus* ENR. *e*, ribbon diagram of the model of the enoyl substrate fitted into the *B. napus* ENR A138G active site. The cofactor molecule, the enoyl, and pantetheine moieties of the enoyl ACP are shown in all-atom representation with the carbon atoms colored *orange* (cofactor) and *black* (substrate). The proposed locations of the growing acyl chain (*R*) and the ACP molecule are marked. Residues 236–246 are shown in *magenta*. The pantetheine moiety of the substrate was modeled using the structure of that in the CoA molecule, as observed in the crystal structure of the citrate synthase complex with CoA and citrate (PDB code 2cts) (26), with the torsion angles adjusted such that there was no steric clash with atoms of the protein. *f*, stereoview of superposition of bound diazaborine and a model for the enoyl substrate. The carbon atoms are colored *orange* in the cofactor and diazaborine molecules and *black* in the substrate model (O, *red*; N, *blue*; S, *yellow*; P, *magenta*; B, *green*). The proposed locations of the growing acyl chain (*R*) and the ACP molecule are marked. (The figures were prepared using MIDAS (23).)

arrangement of the four atoms closest to the boron is tetrahedral in both the ternary complexes. This is similar to the situation with the *E. coli* enzyme and indicates that on diazaborine binding, the boron atom undergoes conversion from sp^2 hybridization state to sp^3 and forms a covalent bond with the 2′ oxygen of the nicotinamide ribose of either NAD^+ or NADH. Superposition of the two ternary complexes based on the overlap of 296 C_α with a root mean square deviation of 0.2 Å shows that, within the limit of the experimental error in the coordinates (0.23 and 0.29 Å for the ENR A138G-NAD^+-diazaborine and the ENR A138G-NADH-diazaborine complexes, respectively, as determined by SIGMAA; Ref. 20), their structures are essentially identical.

Taking into account the results of kinetic studies (4, 10), which indicate that diazaborine acts as an inhibitor of the enoyl reductase in the presence of NAD^+ and not NADH, the energetics of the formation of these two distinct complexes would be expected to be significantly different. Therefore, at first sight the structural similarity of the *B. napus* ENR A138G-NAD^+-diazaborine and the ENR A138G-NADH-diazaborine complexes is surprising. There are currently two possible explanations for this. First, the structures of the ternary complexes might be very similar, but the difference in the oxidation state of the nicotinamide ring for NAD^+ and NADH would result in a distinct difference in the strength of the interactions with the enzyme and diazaborine. Thus, for NAD^+, the charge on the nicotinamide ring, the presence of aromaticity, and the loss of the hydride could influence the affinity of the site for diazaborine. In particular, a possible stabilizing feature could be the full negative charge on the boron of the diazaborine interacting with the oxidized nicotinamide ring. If this is the case, then the difference in affinity is not reflected in any dramatic changes in the structure. Indeed, the only difference of the complex with NADH compared with that with NAD^+ appears to be an apparent increase of 9 and 14 $Å^2$ in the average temperature factors of the nucleotide and diazaborine molecules, respectively, in the NADH complex (Table I). However, at this stage, we attach little significance to this difference since it is small and the lower resolution of the analysis of the complex with NADH and diazaborine precludes accurate refinement of the

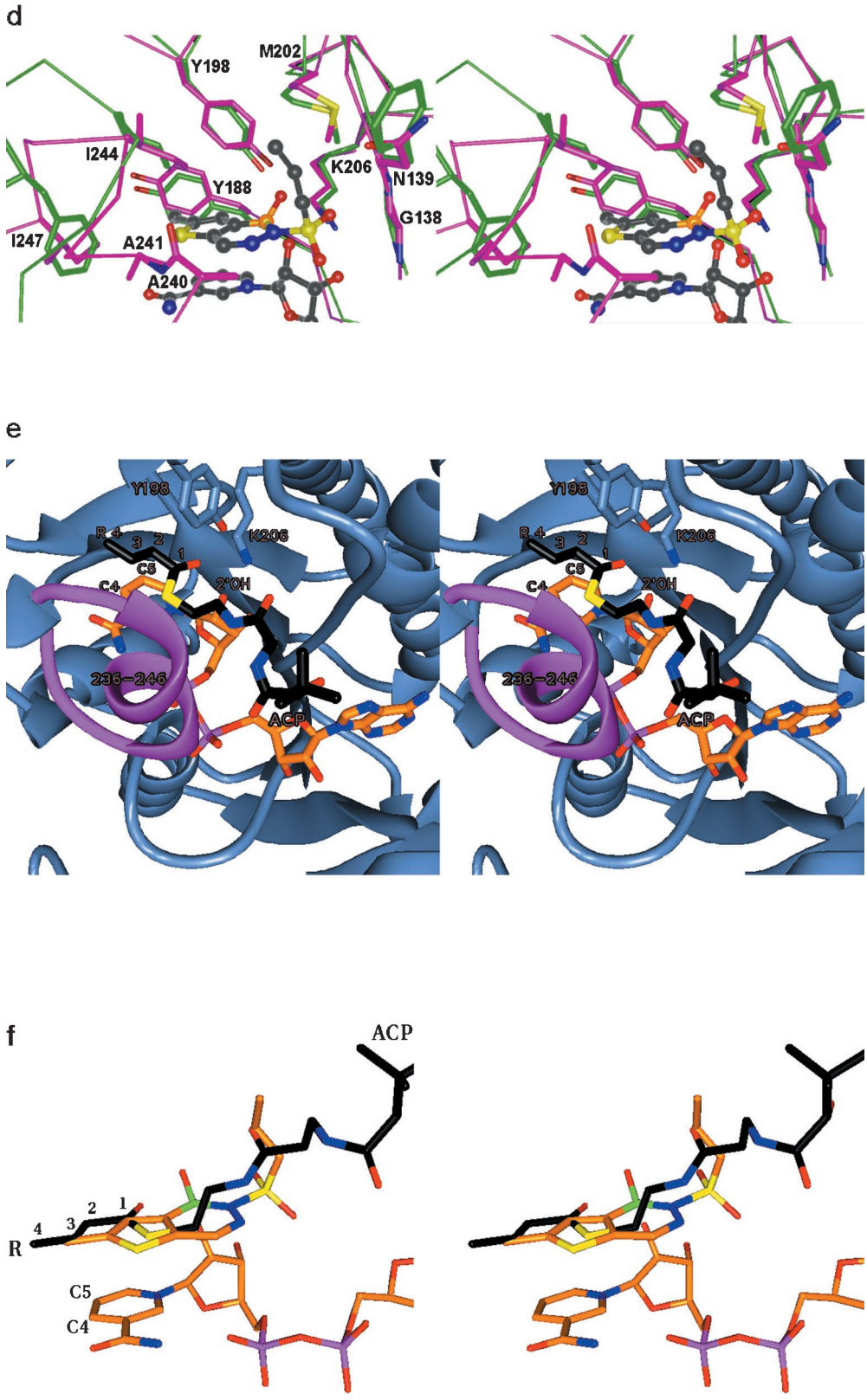

FIG. 2—*continued*

temperature factors. The second possibility is more complicated and arises from the presence in most samples of NADH of contaminating quantities of NAD^+. In the binary complexes of *B. napus* ENR A138G, the identity of the respective oxidized or reduced cofactor in the structures can be inferred from the clear difference in the electron density maps and the ordering of the nicotinamide ring in the complex with NADH. However, for the structures of the two ternary complexes, we cannot preclude the possibility that during the soaking of the crystals of the binary ENR A138G-NADH complex in a solution containing diazaborine and NADH, the NADH initially present in the crystal has been exchanged for contaminating NAD^+, which, while binding to the enzyme with lower affinity than NADH, could be stabilized by the binding of diazaborine. At the

ENR source		Sequence	GenBank accession number
Brassica napus	233	A G P L G S R A A K A I	P80030
E. coli	189	A G P I R T L A A S G I	P29132
M. tuberculosis	191	A G P I R T L A M S A I	P46533
M. avium	190	A G P I R T L A M A G I	O07400
Anabaena sp.	197	A G P I R T L A S S A V	Q05069
Haemophilus influenzae	197	A G P I R T L A A S G I	P44432
Helicobacter pylori	188	A G P I R T L A S S G I	AE001456
Pseudomonas aeruginosa	192	A G P I R T L A A S G I	AF104262
Rickettsia prowazekii	190	A G P I K T L A S S A I	AJ235271
Chlamydia trachomatiss	223	A G P L A S R A G K A I	AE001284
Aquifex aeolicus	204	A G P V K T L A A Y S I	AE000745
Corynebacterium glutamicum	190	A G P N R T L A M S A I	AF050109

FIG. 3. **Sequence comparison of the region surrounding the residues Ser^{238}, Ala^{240}, and Ala^{241} in *B. napus* ENR with other known and putative enoyl reductases.** Highlighted are the functionally conserved residues at positions equivalent to Ser^{238} and Ala^{240} in *B. napus* ENR.

resolution of this study, we cannot expect to distinguish the difference in the structure of the cofactor due to the different nature of the oxidized and reduced states of the nicotinamide ring. Therefore, our current interpretation of the data is complicated by a potential uncertainty concerning the nature of the bound cofactor in the complex with NADH and thienodiazaborine. Further work is needed to clarify this.

Co-crystallization of ENR A138G with NAD$^+$ and Diazaborine Reveals a Substantial Conformational Change in the Protein Active Site—The search for conditions for co-crystallization of the enzyme with both the cofactor and the inhibitor yielded crystals for the ternary ENR A138G-NAD$^+$-thienodiazaborine complex, that grew from a buffered solution of NaCl. These crystals were found to belong to a different space group ($I4_122$). The structure of the complex was determined by the molecular replacement procedure and revealed that the part of the chain comprising the residues 236–246 is significantly shifted from the position observed in the binary complexes with NAD$^+$ or NADH. In the new crystal form, this loop adopts a regular helical conformation, which forms an additional edge of the diazaborine-binding site and makes it less accessible to the solvent (Fig. 2, *a* and *b*). This motion draws the residues Ala^{240} and Ala^{241} closer to the diazaborine so that now both their side-chain and main-chain atoms make extensive van der Waals contacts with the edge of the fused rings of the inhibitor. In addition, the hydroxyl of Ser^{238} now approaches within hydrogen bonding distance of one of the oxygens of the pyrophosphate moiety. Given that diazaborine is thought to mimic the enzyme's natural enoyl substrate (7), these findings provide a potential explanation for the strong conservation of the alanine residue at position 240 of *B. napus* ENR in the aligned sequences of representative enoyl reductases (Fig. 3). Furthermore, at position 238, the ENR sequences show a preference for either serine or threonine, both of which contain a hydroxyl that could interact similarly with the pyrophosphate moiety of the nucleotide cofactor. Overall, this suggests that these two residues are essential for ENR activity and the conformational change of the 236–246 loop seen in the crystal structure of the *B. napus* ENR A138G-NAD$^+$-thienodiazaborine represents a key step in the enzyme's catalytic cycle. This important structural adjustment, which favors the tight binding of both the cofactor and the inhibitor, was not observed when the ternary complex was produced by soaking diazaborine into the crystals of the binary complex of the mutant enzyme with either reduced or oxidized form of the cofactor. One possible explanation for this is that in the crystal form observed for the binary complexes of *B. napus* ENR A138G with NADH or NAD$^+$ the loop 236–246 is involved in crystal packing interactions in which the main-chain carbonyl oxygen of Ala^{241} and peptide nitrogens of Ala^{241} and Lys^{242} make hydrogen bonds with the side-chain amide group of Gln^{70} in a symmetry-related molecule.

Superposition of the structures of *B. napus* ENR A138G co-crystallized with NAD$^+$ and thienodiazaborine and the corresponding wild type *E. coli* ENR co-crystallized complex (PDB code 1dfh) (7) reveals that 204 C_α atoms can be overlapped with a root mean square deviation of 0.9 Å (Fig. 2, *c* and *d*), indicating the overall similarity of the two enzymes, despite there being only 35% sequence identity between them (9). Inspection of the superimposed structures further revealed that the mode of diazaborine binding is remarkably similar, with a large number of conserved residues involved in interaction with diazaborine in *B. napus* ENR A138G and in *E. coli* ENR (in parentheses) as follows: Gly^{138} (Gly^{93}), Tyr^{188} (Tyr^{146}), Tyr^{198} (Tyr^{156}), Met^{202} (Met^{159}), Lys^{206} (Lys^{163}), Ile^{244} (Ile^{200}), and one conservative amino acid substitution (Ile^{247} (Phe^{203})) (Fig. 2*d*). The most noticeable difference between the two structures concerns the position of the 236–246 loop in *B. napus* ENR A138G and the corresponding loop 192–202 in the *E. coli* wild type enzyme. In the structure of the *E. coli* ENR complex with NAD$^+$, this loop is completely disordered (21), whereas in the co-crystal of the *E. coli* ENR with NAD$^+$ and thienodiazaborine it is observed in a well defined position in one of the two subunits in the asymmetric unit. A comparison of the latter structure with that of the co-crystal of *B. napus* ENR A138G with NAD$^+$ and diazaborine shows that the 236–246 loop in the *B. napus* enzyme and the 192–202 loop in the *E. coli* enzyme adopt different conformations (Fig. 2*c*). In contrast to the situation in the *B. napus* ENR A138G complex with NAD$^+$ and diazaborine, where strongly conserved residues Ser^{238} and Ala^{240} make contacts with the NAD$^+$ and inhibitor molecules, the equivalent residues in the structure of the *E. coli* complex (Thr^{194} and Ala^{196}) make no such contacts. However, recent further refinement of the structures of the diazaborine complexes of *E. coli* ENR[2] has revealed that the two subunits in the

[2] C. W. Levy and J. B. Rafferty, personal communications.

asymmetric unit of these crystals adopt different conformations for the 192–202 loop, one of which is closely related to the helical loop structure seen in the *B. napus* ENR A138G.

Together, these data suggest that the flexibility of this part of the structure is essential for the enzyme's function. Furthermore, close contacts of the inhibitor and the strongly conserved residues Ser^{238} and Ala^{240} seen in the structure of *B. napus* ENR A138G co-crystallized with NAD^+ and thienodiazaborine suggest that the helical loop conformation is more likely to represent a catalytically important conformation than that previously reported for the *E. coli* enzyme.

A proposed catalytic mechanism for enoyl ACP reduction by *B. napus* ENR involves hydride transfer from the C4 position of NADH to the C3 carbon atom of the enoyl moiety of the substrate followed by donation of a proton to the oxygen of the resultant enolate anion from the side chain of Tyr^{198} (14). Lys^{206} is thought to be a second catalytic residue, whose amino group might stabilize the negatively charged transition state. Analysis of arrangement of the key residues around the nicotinamide moiety of the cofactor in the ENR active site and the mode of diazaborine binding to ENR allows us to propose a model for the binding of the natural enoyl substrate. In this model (Fig. 2, *e* and *f*), the acyl chain of enoyl ACP is placed above the nicotinamide ring of the cofactor in such a way that the double bond reduced by ENR during catalysis (between the C2 and C3 positions in the enoyl moiety of the substrate) lies over and parallel to the C4-C5 double bond in the nicotinamide ring, with the carbonyl group and the C2, C3, and C4 atoms of the enoyl moiety lying in the plane of the aromatic bicyclic ring of diazaborine. The angle formed between the C3 atom of the enoyl moiety of the substrate and the C4 and N1 atoms of the nicotinamide ring is close to 100°. With this arrangement of the modeled enoyl moiety of the substrate and the nicotinamide ring of the cofactor, the geometry requirements for hydride attack on the natural enoyl substrate are fulfilled (24, 25). The proposed position of the carbonyl oxygen atom of the enoyl moiety is close to that of the boron atom in diazaborine and implies formation of the hydrogen bonds with both the 2′-hydroxyl of the nicotinamide ribose and the phenolic oxygen of catalytic Tyr^{198}. In this mode of binding of the substrate, the pantetheine moiety, covalently attached to the C1 atom of the enoyl moiety of the substrate, would fit into the tunnel formed by the protein residues 139–140, 202, and 240–244 and the atoms of the nicotinamide ribose. Although the conformation of the pantetheine arm of the substrate cannot be unambiguously defined in this model, the general similarity of the substrate to diazaborine strongly suggests that, in the enzyme-substrate complex, the 236–246 loop might adopt a closely related helical conformation, stabilizing the substrate bound to ENR through van der Waals contacts.

Acknowledgments—We thank the support staff at the Synchrotron Radiation Source, Daresbury Laboratory, Warrington, United Kingdom, for assistance with station alignment. We also acknowledge Karin van der Linden and Bets Verbree for technical assistance.

REFERENCES

1. Harwood, J. L. (1988) *Annu. Rev. Plant Physiol. Plant Mol. Biol.* **39,** 101–138
2. Quemard, A., Sacchettini, J. C., Dessen, A., Vilcheze, C., Bittman, R., Jacobs, W. R., Jr., and Blanchard, J. S. (1995) *Biochemistry* **34,** 8235–8241
3. Bergler, H., Wallner, P., Ebeling, A., Leitinger, B., Fuchsbichler, S., Aschauer, H., Kollenz, G., Högenauer, G., and Turnowsky, F. (1994) *J. Biol. Chem.* **269,** 5493–5496
4. Kater, M. M., Koningstein, G. M., Nijkamp, H. J. J., and Stuitje, A. R. (1994) *Plant Mol. Biol.* **25,** 771–790
5. Levy, C. W., Roujeinikova, A., Sedelnikova, S., Baker, J. B., Stuitje, A. R., Slabas, A. R., Rice, D. W., and Rafferty, J. B. (1999) *Nature* **398,** 383–384
6. McMurry, L. M., Oethinger, M., and Levy, S. B. (1998) *Nature* **394,** 531–532
7. Baldock, C., Rafferty, J. B., Sedelnikova, S. E., Baker, P. J., Stuitje, A. R., Slabas A. R., Hawkes, T. R., and Rice, D. W. (1996) *Science* **274,** 2107–2110
8. Turnowsky, F., Fuchs, K., Jeschek, C., and Högenauer, G. (1989) *J. Bacteriol.* **171,** 6555–6565
9. Kater, M. M., Koningstein, G. M., Nijkamp, H. J. J., and Stuije, A. R. (1991) *Plant Mol. Biol.* **17,** 895–909
10. de Boer, G.-J., Pielage, G. J. A., Nijkamp, N. I. J., Slabas, A. R., Rafferty, J. B., Baldock, C., Rice, D. W., and Stuitje, A. R. (1999) *Mol. Microbiol.* **31,** 443–450
11. Howard, A. J., Nielsen, C., and Xuong, N. H. (1985) *Methods Enzymol.* **114,** 452–472
12. Otwinowski, Z., and Minor, W. (1997) *Methods Enzymol.* **276,** 307–326
13. Collaborative Computational Project No. 4. (1994) *Acta Crystallogr. Sect. D* **50,** 760–763
14. Rafferty, J. B., Simon, J. W., Stuitje, A. R., Slabas, A. R., Fawcett, T., and Rice, D. W. (1995) *Structure* **3,** 927–938
15. Tronrud, D. E. (1992) *Acta Crystallogr. Sect. A* **48,** 912–916
16. Moews, P. C., and Kretsinger, R. H. (1975) *J. Mol. Biol.* **91,** 201–228
17. Jones, T. A. (1978) *J. Appl. Crystallogr.* **11,** 268–270
18. Laskowski, R. A., MacArthur, M. W., Moss, D. S., and Thornton, J. M. (1993) *J. Appl. Crystallogr.* **26,** 283–291
19. Navaza, J. (1994) *Acta Crystallogr. Sect. A* **50,** 157–163
20. Read, R. J. (1986) *Acta Crystallogr. Sect. A* **42,** 140–149
21. Baldock, C., Rafferty, J. B., Stuitje, A. R., Slabas, A. R., and Rice, D. W. (1998) *J. Mol. Biol.* **284,** 1529–1546
22. Jones, T. A., Zou, J.-Y., Cowan, S. W., and Kjeldgaard, M. (1991) *Acta Crystallogr. Sect. A* **47,** 110–119
23. Ferrin, T. E., Huang, C. C., Jarvis, L. E., and Langridge, R. (1988) *J. Mol. Graphics* **6,** 13–27
24. Burgi, H. W., and Dunitz, J. D. (1983) *Acc. Chem. Res.* **16,** 153–161
25. Wilkie, J., and Williams, I. H. (1995) *J. Chem. Soc. Perkin Trans.* **2,** 1559–1567
26. Remington, S., Wiegand, G., and Huber, R. (1982) *J. Mol. Biol.* **158,** 111–152